

Superconductivity in doped picene

A. Subedi and L. Boeri

Studying carbon, with its many allotropes and compounds, is one of the most fascinating problems in science. To mention only physics, before graphene, which was awarded the Nobel prize in 2010 opening exciting perspectives for fundamental and applied research, many other systems, such as nanotubes, fullerenes and intercalated graphites have played an important role in several fields, including superconductivity. The most recent discovery is a new class of *aromatic superconductors*, comprising molecular crystals doped with alkali or alkaline earths. These are *polycyclic aromatic hydrocarbons*, *i.e.* planar molecules formed by a number of juxtaposed hexagonal benzene rings (C_6H_6). The first report of superconductivity regarded picene doped with potassium (K) and rubidium (Rb), with a maximum critical temperature (T_c) of 18 K; after that, superconductivity was also found in phenanthrene and coronene doped with K ($T_c=5K$ and 15 K), phenanthrene doped with strontium (Sr) and barium (Ba) ($T_c=5.6-5.8$ K) and 1,2:8,9-dibenzopentacene - $C_{30}H_{18}$ ($T_c=33$ K) doped with K.[1]

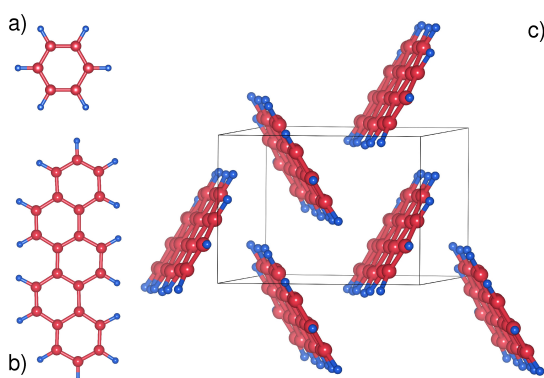


Figure 1: (a): A benzene ring (C_6H_6) is the main building block of alternant polycyclic aromatic hydrocarbons, such as picene, phenanthrene, coronene, which superconduct when intercalated with alkali or alkali metals. (b): The picene molecule ($C_{22}H_{14}$) is formed by five rings, juxtaposed in an armchair fashion; it can also be seen as a small fragment of H-terminated graphene. (c): In the crystal, the molecules are arranged in a herringbone fashion in the (a, b) plane, and stacked along the c direction. The unit cell is monoclinic and contains two formula units. The figure shows a side view.

At the moment, the nature and range of parameters for superconductivity in intercalated hydrocarbons is strongly debated; it is however clear that they are strongly related to two families of carbon superconductors: graphite intercalation compounds (GICs), which are conventional, BCS-like superconductors [2] and alkali-doped fullerenes (A_3C_{60}), which instead have a rich phase diagram determined by a non-trivial interplay between strong local electron-phonon (ep) and on-site Coulomb correlations in a highly non-adiabatic regime. [3]

In this work, we performed first-principles calculations of the electronic structure, phonon and ep interaction of doped picene in the rigid band approximation (RBA), using Density Functional Perturbation Theory (DFPT), complementing previous theoretical and experimental studies which have focused on electronic properties and correlations. We showed that picene, and most likely other intercalated hydrocarbons, belongs to the same class of strongly correlated ep superconductors as the fullerenes, for which a local approach that includes both the ep coupling and Coulomb correlations on an equal footing is more appropriate than the standard Migdal Eliashberg (ME) approach. [4]

Picene ($C_{22}H_{14}$) is a polycyclic aromatic hydrocarbon formed by five benzene rings in an armchair arrangement - Fig. 1 ($a - b$). Solid picene is an insulator, with a gap of ~ 3.3 eV, which can form in either monoclinic or orthorhombic structure; the superconducting samples, with an average doping of $x = 3$ K or Rb atoms per molecule ($K/Rb_xC_{22}H_{14}$) are also monoclinic ($P2_1$ space group). The unit cell contains two picene molecules placed in a herringbone arrangement in the (a, b) plane which are then stacked along c direction - Fig. 1 (c). The shortest intermolecular C-C distance is 3.5 Å within the xy plane and 3.9 Å along z , which are more than twice the typical intramolecular nearest-neighbour C-C distance of 1.4 Å. In the doped superconducting crystals, the a axis expands while the b and c axes shrink. It is inferred from this that the dopants most likely occupy intra-layer positions since inter-layer intercalation would have caused the c axis to expand. However, the detailed experimental structure of doped picene, including the precise determination of doping, is not available. For this reason, we simulated the effect of doping using the rigid band approximation (RBA) and did not include explicitly the dopants in the calculations; we performed calculations in the monoclinic $P2_1$ structure of undoped picene, [1] relaxing the the internal coordinates; this yielded a dynamically stable structure, with real phonon frequencies.

Our calculated electronic structure agrees well with previous DFT calculations;[4] in undoped picene, a gap of ~ 2.4 eV separates the bonding valence bands from the anti-bonding conduction bands which, in an energy range

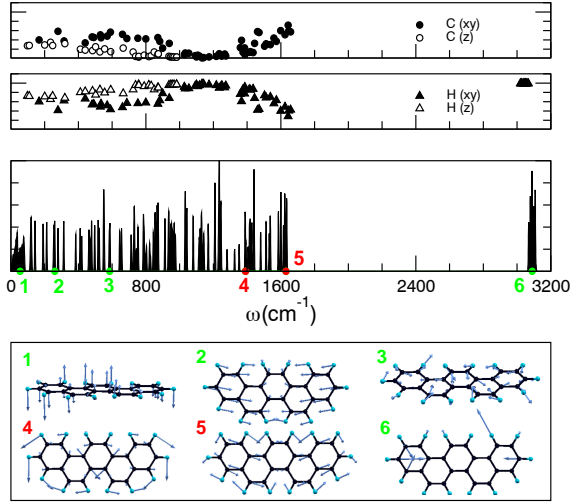


Figure 2: Vibrational properties of solid picene. *From top to bottom*: Partial C and H contribution to the phonon eigenvectors of a picene molecule. Phonon DOS of (undoped) solid picene. The numbers mark the energy positions of selected modes, whose Γ -point eigenvectors are shown in the bottom panel. (1) low-frequencies out-of-plane, bending modes ($\omega \sim 55 \text{ cm}^{-1}$); (2) and (3), breathing modes, with $\omega \sim 260$ and $\sim 585 \text{ cm}^{-1}$; (4) and (5), C-H bending and C-C bending and stretching modes ($\omega \sim 1390$ and $\sim 1625 \text{ cm}^{-1}$); (6) high energy in-plane C-H bond stretching modes ($\omega \sim 3200 \text{ cm}^{-1}$).

Modes 4 and 5, in red, give the highest contribution to the ep coupling, shown in Fig. 3.

of $\sim \pm 3 \text{ eV}$ around the middle of the gap, have mostly C p_z character. They are lumped into small subsets with very small in- and out-of-plane dispersion reflecting the molecular nature of the solid. In superconducting picene (K/Rb $_{3.3}$ C $_{22}$ H $_{14}$) the ~ 3 electrons donated from the alkali atoms to each molecule populate a subset of 4 bands immediately above the gap. These bands have a total bandwidth of $\sim 0.3 \text{ eV}$ and derive from a combination of the two lowest unoccupied molecular orbitals (LUMO and LUMO+1), which have a small energy separation of $\sim 66 \text{ meV}$ in the molecule. The energy separation between the two highest occupied molecular orbitals (HOMO and HOMO-1) is instead higher ($\sim 170 \text{ meV}$) so that the four corresponding bands in the solid are grouped in two subsets of two bands separated by a gap of $\sim 0.1 \text{ eV}$. In our work, we have studied within the RBA the effect of doping electrons or holes into the states immediately above (LUMO*) and below (HOMO) the gap.

For all dopings, we used the phonon spectrum of undoped solid picene, whose properties are summarized in Fig. 2. Most of the phonon branches of solid picene have very little dispersion, which reflects the molecular nature of the solid. The dispersive intermolecular modes (acoustic, translations and rotations of picene molecules) make up most of the phonon Density of States (DOS) for frequencies below $\sim 85 \text{ cm}^{-1}$. The remaining modes are intramolecular vibration of carbon (C) and hydrogen (H) atoms and their general character can be inferred from the top two panels of Fig. 2, which show the calculated partial eigenvectors of an isolated picene molecule. The modes below $\sim 800 \text{ cm}^{-1}$ are due to in- and out-of-plane vibrations involving both C and H atoms that cause only small changes in the bond length between neighbouring atoms. The vibrations between $\sim 800 \text{ cm}^{-1}$ and $\sim 1300 \text{ cm}^{-1}$ are mostly out-of-plane, while the modes between $\sim 1300 \text{ cm}^{-1}$ and $\sim 1600 \text{ cm}^{-1}$ have C-H bending and C-C bending and stretching character. The spectral distribution of modes in this region is very similar to that of graphene and (intercalated) graphites. The modes very high in energy ($\sim 3200 \text{ cm}^{-1}$) have in-plane C-H bond stretching character. Representative examples for each class are shown in the bottom panel of Fig. 2.

Fig. 3 summarizes the results of calculations of the ep coupling for hole and electron doped picene, which we have used to evaluate the contributions of phonons to the superconducting pairing. The procedure we have used is non-standard, due to the large size of the system (72 atoms/unit cell). In fact, the estimate of the two fundamental quantities in the Migdal-Eliashberg theory for ep superconductivity, *i.e.* the ep Eliashberg spectral function $\alpha^2 F(\omega)$ and for its inverse moment, $\lambda = 2 \int_0^\infty d\omega \alpha^2 F(\omega)/\omega$, require dense grids in reciprocal space for in \mathbf{k} - (electrons) and \mathbf{q} - (phonons) space integration, which is unfeasible for systems that contain more than 8-10 atoms. However, in doped picene we could perform the calculation with affordable grids in momentum space, exploiting the molecular nature of the crystal. [4] We found indeed that, due to the weak momentum dependence of the ep matrix elements, it is possible to factorize the dimensionless ep coupling parameter λ as $\lambda = N(E_F)V_{ep}$, where the density of states $N(E_F)$ is determined by intermolecular interactions and the ep coupling strength V_{ep} is essentially an intramolecular quantity. Similarly, it is possible to define a spectral function for the ep coupling strength V_{ep} , $\bar{\alpha}^2 F(\omega) = \alpha^2 F(\omega)/N(E_F)$. The two intramolecular quantities $\bar{\alpha}^2 F(\omega)$ and V_{ep} converge much faster as a function of \mathbf{k} -mesh than the intermolecular $N(E_F)$. To eliminate the noise coming from pathological regions of the DOS, we evaluated V_{ep} and $\bar{\alpha}^2 F(\omega)$ for different fillings x of the electronic bands, as shown in the two insets of Fig. 3; here red and blue refer to doping with holes ($-x$) and electron ($+x$), respectively. The values of V_{ep} thus determined are fairly constant with x within a single subset of bands, as one would expect for an intramolecular quantity. We obtain $V_{ep} = 150 \pm 20 \text{ meV}$ for holes and $V_{ep} = 110 \pm 5 \text{ meV}$ for electrons.

Before discussing the implications for superconductivity, it is insightful to analyze the V_{ep} spectral function

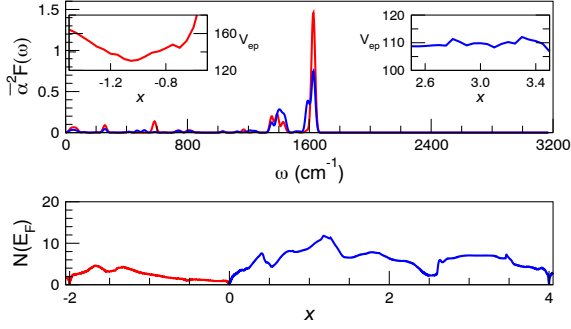


Figure 3: (Color online) *Upper Panel*: Spectral distribution of the ep matrix elements of solid picene, doped with holes (red) or electrons (blue). The two insets show the doping dependence of the corresponding ep coupling strength $V_{ep} = \int \omega^{-1} \bar{\alpha}^2 F(\omega) d\omega$ for different values of doping x . *Lower Panel*: Electronic DOS per picene molecule, in states/(meV spin) as a function of doping x . The total ep coupling constant λ as a function of doping is given by $\lambda(x) = N(x)V_{ep}$.

$\bar{\alpha}^2 F(\omega)$, which is shown in the upper panel of Fig. 3. The V_{ep} spectral function has two main peaks at ~ 1400 cm^{-1} and ~ 1600 cm^{-1} , which correspond to modes that bend C-H bonds and stretch C-C bonds (modes **4** and **5** in Fig. 2). Additionally, we also find smaller coupling to modes lower frequencies ($\omega < 800$ cm^{-1}). Our estimate of the coupling excludes two contributions: that of modes below 100 cm^{-1} , which are explicitly excluded in the integration of λ , because they are not *intra*-molecular modes, and thus require a more careful \mathbf{q} - and \mathbf{k} - integration, and the effect of the dopants - Rb,K - which cannot be treated in our RBA. In graphite intercalation compounds (GICs), where there is a substantial contribution of intercalant character to states near the Fermi level, the dopants reduce the ep coupling to carbon bond stretching modes, but also provide some additional coupling to low-lying Einstein phonons. [2] These two effects balance each other to leave λ basically unchanged, while ω_{in} is reduced due to the additional weight at low frequencies. We expect a similar effect in the case of picene, although smaller in magnitude.

Accurate values of $\lambda = V_{ep}N(E_F)$ as a function of doping in picene can be obtained using the DOS shown in the lower panel of Fig. 3, which has been obtained using a $(8)^3$ \mathbf{k} -grid and tetrahedron method. For $x = 3$, we get $N(E_F) = 7.06$ states $\text{spin}^{-1} \text{meV}^{-1}$, $\lambda = 0.78$ and $\omega_{\text{in}} = 1021$ cm^{-1} . Using $\mu^* = 0.12$ and the McMillan formula for T_c , as it is commonly done to obtain a reasonable estimate of the T_c for conventional superconductors, we obtain a critical temperature $T_c = 56.5$ K, which is more than three times the experimental value. Reasons and consequences of this discrepancy are discussed below. In the case of hole doping, the T_c 's are lower due to smaller values of DOS. For $x \sim -1.33$, with the same value of $\mu^* = 0.23$, $N(E_F) = 4.31$ states $\text{spin}^{-1} \text{meV}^{-1}$, $\lambda = 0.65$ and $\omega_{\text{in}} = 890$ cm^{-1} , and we obtain a maximum T_c of 6 K.

These relatively high McMillan T_c 's that result from strong ep coupling to a few high-energy carbon bond-stretching phonons indicates that superconductivity in alkali-doped picene and other hydrocarbons is most likely phonon-mediated, and related to that of other superconductors that contain carbon and boron, such as MgB_2 , boron-doped diamond, and GICs. This first conclusion is confirmed by two other calculations of the ep coupling of doped picene, using different approximations - RBA and frozen-phonons, and linear response with Wannier functions for the a metastable LDA structure of $\text{K}_3\text{C}_{22}\text{H}_{14}$ - which have appeared in literature after our work. [4] All calculations find a similar magnitude of the coupling, but a different spectral distribution (the calculation which includes dopants finds a \mathbf{q} -dependent coupling associated to the low-energy intercalant phonons).

However, it is important to stress that the estimates of T_c based on Migdal-Eliashberg theory must be taken with care in this case. In fact, we have seen that the bandwidth of the conduction bands ($W \sim 300$ meV for electrons and ~ 1 eV for holes), the frequencies of strongly coupled phonons ($\omega_{ph} \sim 200$ meV), the ep coupling strength ($V_{ep} \sim 110$ - 150 eV), all have similar magnitudes, close also to that of Coulomb repulsion ($U \sim 1.2$ eV), estimated by other authors. In this range of parameters, the two most important approximations in Migdal-Eliashberg theory of superconductivity, Migdal's theorem and the Morel-Anderson scheme for the screening of the Coulomb repulsion, are invalid. In fullerenes, this regime of parameters gives rise to a variety of interesting phenomena, the most spectacular being the occurrence of ep superconductivity near a Mott insulating phase, well captured by theoretical studies of local models of interacting phonons and electrons in the non-adiabatic regime. [3] Intercalated picene, and other intercalated hydrocarbons, are also a strong candidates for this kind of strongly correlated, non-adiabatic ep superconductivity. The experimental situation is still premature to verify this claim, but several tests are possible for this hypothesis. For example, Migdal-Eliashberg theory would predict a smooth behaviour of superconductivity as a function of doping and pressure that is governed essentially by the value of the electronic DOS at the Fermi level. On the other hand, strongly correlated local models would predict a phase diagram where superconductivity exists in close proximity to a possible Mott insulating state, which could be tuned by doping or by a change in the intermolecular hopping driven by pressure or intercalation of isovalent atoms with different sizes. A very exciting prospect is the possibility of studying a wider range of intercalated hydrocarbons by changing the number and arrangement of benzene rings. This could be an interesting avenue

for independently tuning the ep coupling and bandwidth and degeneracy of the conduction bands and obtaining an extensive mapping of the parameter space for strongly correlated ep superconductors. The recent reports of superconductivity in other intercalated hydrocarbons, are very encouraging in this sense.[1]

References:

- [1] R. Mitsuhashi et al., *Nature* **464**, 76 (2010); X. F. Wang et al., *Nat. Commun.* **2**, 507 (2011); X. F. Wang et al., *arXiv:1110.5458*; Y. Kubozono et al., *Phys. Chem. Chem. Phys.* **13**, 16476 (2011); M. Xue, et al., *ArXiv:1111.0820*.
- [2] T. E. Weller et al., *Nature Physics* **1**, 39 (2005); N. Emery et al., *Phys. Rev. Lett.* **95**, 087003 (2005); J. S. Kim et al., *Phys. Rev. Lett.* **99**, 027001 (2007).
- [3] A.F. Hebard et al., *Nature* **350**, 600 (1991); O. Gunnarsson, *Alkali-Doped Fullerenes*, World Scientific, Singapore, 2004; A.Y. Ganin et al., *Nature Mater.* **7**, 367 (2008); M. Capone et al., *Rev. Mod. Phys.* **81**, 943 (2009).
- [4] A. Subedi and L. Boeri, *Phys. Rev. B* **84**, 020508(R) (2011); see also: M. Casula et al., *Phys. Rev. Lett.* **107**, 137006 (2011); T. Kato, et al., *Phys. Rev. Lett.* **107**, 077001 (2011).